Supporting Information

Insights into Regional Wetting Behaviors of Amphiphilic Collagen for Dual Separation of Emulsions

Guangyan Chen,[a] Baicun Hao,[a] Yujia Wang,[a] Yanan Wang,[a] Hanzhong Xiao,[a] Huifang Li,[a] Xin Huang,*[a] Bi Shi[a]

[a] National Engineering Research Center of Clean Technology in Leather Industry, Sichuan University, Chengdu 610065, P.R. China.

E-mail: xhuangscu@163.com (X. Huang)

Emulsion separation

A column separation apparatus (shown in Schematic illustration S1) was used for emulsion separation, and the inner diameter of column was 10.0 mm. 1.5 g of collagen fibers without pre-wetting were packed into the column. Then, emulsion was pumped into the column through the plastic tube by the peristaltic pump, and the filtrates were collected by the automatic collector.

Besides, 1.5 g of collagen fibers was immersed in 30 mL of n-dodecane, kerosene, petroleum ether and water, respectively. After this, the n-dodecane (kerosene, petroleum ether, water) pre-wetted collagen fibers were packed into the column, and then used for the separation of corresponding emulsion (n-dodecane pre-wetted collagen fibers for E1 and E4, kerosene pre-wetted collagen fibers for E2, petroleum ether pre-wetted collagen fibers for E3, and water pre-wetted collagen fibers for E5, E6 and E7) according to the similar procedure mentioned above.

The separation flux was calculated as $V/(S \cdot t)$, where t was the separation time (h), V and S were the volume (L) of the filtrates collected in the time of t and the inner cross-section area of column (0.0785 m^2), respectively.

The separation efficiency (%) was determined by calculating oil/water purity in the filtrate, which was calculated as $100\%-C$, where C was the water/oil weight percentage of the filtrate.[1-2]

Long-term stability and reusability

The long-term stability and reusability of collagen fibers were investigated by the separation of E1 using the similar separation procedures mentioned above. Specifically, E1 was

separated by collagen fibers for the first cycle with a total time of 1.0 h. After being flushed with anhydrous alcohol and dried at 50^{o}C in air, the re-generated collagen fibers were reused for the next separation cycle. For each cycle, the separation flux and separation efficiency were calculated per 3.0 min.

Water content measurement

Water content was determined by an Oxidation-Reduction method of Karl Fischer titration. Briefly, a certain volume of methanol or ethanol was placed in the titration cell of the Karl Fischer titrator that contains two identical Pt electrodes, in which the methanol or ethanol submerged the Pt electrodes. The pre-titration was carried out with Karl Fischer agent for the removal of water in methanol or ethanol. Then, the oily filtrate was weighted and rapidly added into the above titration cell and further titrated with Karl Fischer agent. The titration was completed when the current value between the two electrodes reached to 50.0 A. The water content in the oily filtrate was determined by the quality of Karl Fischer agent consumed.

Oil content measurement

Oil content in the aqueous filtrate was measured by infrared photometric method. Briefly, 100 mL of aqueous filtrate was transferred to a separatory funnel, and adjusted the pH of aqueous filtrate to 1.0 with HCl solution. Then, a total volume of 25 mL of C_2Cl_4 was added into the separatory funnel and shaken for three minutes, followed by setting for a while. When the C_2Cl_4 phase and water phase were layered, the C_2Cl_4 was collected from the bottom of the separatory funnel, and followed by the adsorption of water contained in C_2Cl_4 with excessive

anhydrous sodium sulfate. The oil content was obtained by measuring the absorbance of collected C_2Cl_4 at 2930, 2960 and 3030 cm^{-1} on an infrared photometer oil content analyzer.

Molecular dynamics simulations

The collagen fiber model was built based on the bovine Type I collagen molecules (tropocollagen), which is complied with the four levels of hierarchical structures of fibrillar collagen protein, including the amino acid sequence of α-chain (the primary structure), α-helix of α-chain (the secondary structure), right-handed triple helix of α-chains (the tertiary structure), the quasi-hexagonal arrangement and the right-handed supertwisted structure (the quaternary structure).[3-6] The bovine Type I collagen molecule is composed of two identical α_1 chains and an α_2 chain (Uniport protein database, Swiss-Prot: P02453 and P02465), with the α_1 chain length of 1463 amino acids and the α_2 chain length of 1364 amino acids, respectively. Both α_1 and α_2 polypeptide chains contain signal peptides, N-terminal, helical regions and C-terminal. Herein, we selected the helical regions of α_1 and α_2 chains of bovine Type I collagen molecule as the primary structure to construct the collagen fiber model (Schematic illustration S2). All of the selected amino acid sequences were listed in Table S2. Five polypeptide fragments of α_1 chain were selected and denoted as F_{11}, F_{12}, F_{13}, F_{14}, F_{15}, respectively, while five polypeptide fragments of α_2 chain were selected and denoted as F_{21}, F_{22}, F_{23}, F_{24}, F_{25}, respectively. Each of the selected polypeptide fragments had the length of 81 amino acids. To imitate the quarter-staggered arrangement of type I collagen molecule, the selected polypeptide fragments of F_{11}, F_{12}, F_{13}, F_{14}, F_{15} had an interval of the length of 243 amino acids (~67 nm) between two adjacent fragments. Similarly, the selected polypeptide fragments of F_{21}, F_{22}, F_{23}, F_{24}, F_{25} also had an interval of the length of 243 amino acids

between two adjacent fragments. In these selected polypeptide fragments, a part of proline (P) and lysine (K) (bold letters labeled with underline in the Table S2) were converted to hydroxyproline and hydroxylysine complied with enzymatic posttranslational hydroxylation through Amber 99SB-ILDN parameter force field.

Schematic illustration S3 shows the 4 steps of construction process of the collagen fiber model. Step 1 is to construct fifteen polypeptide chains with left-handed helix (the secondary structure) by using the amino acid sequences of above selected polypeptide fragments of α_1 and α_2 chains of bovine Type I collagen molecule. The step 2 is to construct the right-handed triple helices (the tertiary structure) comprised of three of above polypeptide chains. For example, two incidental polypeptide chains built by the sequences of F_{11} and one polypeptide chain built by the sequences of F_{21} were twisted together into a right-handed triple helix, forming the simulated collagen molecule 1, denoted as RTH1 (Table S2). Similarly, the other four right-handed triple helices of RTH2, RTH3, RTH4, RTH5 were also constructed by twisting their corresponding polypeptide chains built from the selected amino acid sequences (Table S2), respectively. In the step 3, five right-handed triple helices of RTH1, RTH2, RTH3, RTH4, RTH5 were further packed, with the formation of a supertwisted right-handed microfibril (the quaternary structure). In the step 4, four identical supertwisted right-handed microfibrils were bundled to form the collagen fiber model, in which all the right-handed triple helices were packed with a quasi-hexagonal arrangement (the quaternary structure). During the construction process, energy minimization was performed at each step *via* the AMBER force field.

We carried out different MD simulations, including the simultaneous wetting of water (300) and n-dodecane (300) molecules on the collagen fiber model (simulation 1), the simultaneous wetting of water (300) and n-dodecane (1162) molecules on the collagen fiber model (simulation 2) and the simultaneous wetting of water (52926) and n-dodecane (300) molecules on the collagen fiber model (simulation 3). All the all-atom MD simulations were based on a general AMBER force field with the RESP charges and were carried out using the Gromacs-4.6.7 software package.[7-9] The system is a relaxed liquid configuration at 298 K. The total run time was 20 ns NPT for the equilibrium MD simulation. The relaxed system was used as a starting configuration. As it is prior to system relaxation, energy minimization was carried out with a composite protocol of steepest descent using termination gradients of 100 kJ mol^{-1} nm^{-1}. The Nosé-Hoover thermostat was used to maintain the equilibrium temperature at 298 K and the periodic boundary conditions were imposed on all three dimensions.[10] The Particle Mesh-Ewald method was used to compute long-range electrostatics within a relative tolerance of $1x10^{-6}$.[11,12] A cut-off distance of 1.0 nm was applied to real-space Ewald interactions, and the same value was used for van der Waals interactions. The LINCS algorithm was applied to constrain bond lengths of hydrogen atoms.[13] A leap-frog algorithm was used with a time step of 1.0 fs.[14]

Besides the above collagen fiber model, a simplified collagen fiber model was also constructed without the quaternary structure of type I collagen, including the quasi-hexagonal arrangement and right-handed supertwisted structure. As illustrated in the Schematic illustration S4, three polypeptide fragments in the helical regions of α_1 chain of bovine Type I collagen molecule were selected and denoted as F_{16}, F_{17}, F_{18}, respectively, while three

polypeptide fragments in the helical regions of α_2 chain of bovine Type I collagen molecule were selected and denoted as F_{26}, F_{27}, F_{28}, respectively. Each of the selected polypeptide fragments had the length of 81 amino acids. Similarly, the selected polypeptide fragments of F_{16}, F_{17}, F_{18} had an interval of the length of 243 amino acids (~67 nm) between two adjacent fragments. The selected polypeptide fragments of F_{26}, F_{27}, F_{28} also had an interval of the length of 243 amino acids between two adjacent fragments. The corresponding amino acid sequences were listed in Table S3, where a part of the proline (P) and lysine (K) (bold letters labeled with underline in the Table S3) were hydroxylated.

Schematic illustration S5 shows the 3 steps of construction process of the simplified collagen fiber model. The step 1 is to construct nine polypeptide chains (the secondary structure) with left-handed helix using the amino acid sequences (the primary structure) of above selected polypeptide fragments of α_1 and α_2 chains of bovine Type I collagen molecule (Table S3). The step 2 is to build the right-handed triple helices (the tertiary structure). Specifically, two identical polypeptide chains built by F_{16} and one polypeptide chain built by F_{26} were twisted together into a right-handed triple helix, forming the RTH6. The right-handed triple helices of RTH7 were constructed by twisting two identical polypeptide chains built by F_{17} and one polypeptide chain built by F_{27}, while the right-handed triple helices of RTH8 were constructed by twisting two identical polypeptide chains built by F_{18} and one polypeptide chain built by F_{28}. The step 3 is to parallelly arrange the RTH6, RTH7 and RTH8 in two concentric squares, forming the simplified collagen fiber model. For the simplified collagen fiber model, one RTH6 was located in the center of square, eight identical RTH7 were located around four sides of the inner square, and twelve identical RTH8 were

arranged around four sides of the external square, respectively. Energy minimization was also performed at each step of construction *via* the AMBER force. Different MD simulations were carried out on the simplified collagen fiber model, including the simultaneous wetting of water (300) and n-dodecane (300) molecules on the simplified model (simulation 4), the simultaneous wetting of water (300) and n-dodecane (2745) molecules on the simplified model (simulation 5) and the simultaneous wetting of water (67105) and n-dodecane (200) molecules on the simplified model (simulation 6).

Reference:

(1) Yun, J.; Khan, F. A.; Baik, S. Janus Graphene Oxide Sponges for High-purity Fast Separation of Both Water-in-Oil and Oil-in-Water Emulsions. ACS Appl. Mater. Inter., **2017**, 9, 16694-16703.

(2) Zhang, W.; Shi, Z.; Zhang, F.; Liu, X.; Jin, J.; Jiang, L. Superhydrophobic and Superoleophilic PVDF Membranes for Effective Separation of Water-in-Oil Emulsions with High Flux. Adv. Mater., **2013**, 25, 2071-2076.

(3). Jee, S. E.; Zhou, J.; Tan, J., Breschi, L.; Tay, F. R.; Gregoire, G.; Pashley, D. H.; Jang, S. S. Investigation of Ethanol Infiltration into Demineralized Dentin Collagen Fibrils Using Molecular Dynamics Simulations. *Acta Biomater.* **2016**, 36, 175-185.

(4). Gautieri, A.; Vesentini, S.; Redaelli, A.; Buehler, M. J. Hierarchical Structure and Nanomechanics of Collagen Microfibrils from the Atomistic Scale up. *Nano Lett.,* **2011**, 11, 757-766.

(5). Orgel, J. P. R. O.; Irving, T. C.; Miller, A.; Wess, T. J. Microfibrillar Structure of Type I Collagen in Situ. *P. Natl. Acad. Sci. U. S. A.* **2006**, 103, 9001-9005.

(6). Orgel, J. P. R. O.; Antonio, J. D. S.; Antipova O. Molecular and Structural Mapping of Collagen Fibril Interactions. *Connect. Tissue Res.* **2011** 52, 2-17.

(7). Wang, J. M.; Wolf, R. M.; Caldwel, J. W.; Kollman P. A.; Case, D. A. Development and Testing of a General Amber Force Field. *J. Comput. Chem.* **2004**, 25, 1157-1174.

(8). Bayly, C. I.; Cieplak, P.; Cornell, W. D.; Kollman, P. A. A Well-behaved Electrostastatic Potential Based Method Using Charge Restranints for Derixing Atomic Charges: the RESP Model. *J. Phys. Chem.* **1993,** 97, 10269-10280.

(9). Hess, B.; Kutzner, C.; Van Der Spoel, D.; Lindahl, E. Gromacs: Algorithms for Highly Efficient, Load-balanced, and Scalable Molecular Simulation. *J. Chem. Theory Comput.* **2008**, 4, 435-47.

(10). Berendsen, H. J. C.; Postma, J. P. M.; Vangunsteren, W. F.; Dinola, A.; Haak, J. R. Molecular Dynamics with Coupling to an External Bath. *J. Chem. Phys.* **1984**, 81, 3684-3690.

(11). Essmann, U.; Perera, L.; Berkowitz, M. L.; Darden, T.; Lee, H.; Pedersen, L. G. A. Smooth Particle Mesh Ewald Method. *J. Chem. Phys.* **1995**, 103, 8577-8593.

(12). Astrakas, L. G.; Gousias, C.; Tzaphlidou, M. Structural Destabilization of Chignolin Under the Influence of Oscillating Electric Fields. *J. Appl. Phys.* **2012**, 111, No. 074702.

(13). Hess, B.; Bekker, H.; Berendsen, H. J. C.; Fraaije, J. LINCS: A Linear Constraint Solver for Molecular Simulations. J. *Comput. Chem.* **1997**, 18, 1463-1472.

(14). Van Gunsteren, W. F.; Berendsen, H. J. C. A Leap-frog Algorithm for Stochastic Dynamics. *Molecular Simulation Mol. Simulat.* **1988**, 1, 173-185.

Table S1 The constituents of the water-in-oil emulsions (E1, E2, E3, E4) and oil-in-water emulsions (E5, E6, E7).

Emulsion	Span-80 (g)	Water (mL)	n-dodecane (mL)	Kerosene (mL)	Petroleum ether (mL)	Gasoline (mL)
E1	0.8	5.0	500	0	0	0
E2	0.8	5.0	0	500	0	0
E3	0.8	5.0	0	0	500	0
E4	5.0	25	500	0	0	0
E5	0	500	5.0	0	0	0
E6	0	500	0	5.0	0	0
E7	0	500	0	0	0	5.0

Table S2 The polypeptide fragments of F_{11}, F_{12}, F_{13}, F_{14}, F_{15} selected from α_1 chain of bovine Type I collagen (Uniport protein database, Swiss-Prot: P02453 and P02465), the polypeptide fragments of F_{21}, F_{22}, F_{23}, F_{24}, F_{25} selected from α_2 chain of bovine Type I collagen (Uniport protein database, Swiss-Prot: P02453 and P02465).

	F_{11}	α_1	178	188	198	208
			GPMGPSGPRG	L**P**GP**P**GA**P**GP	QGFQGP**P**GE**P**	GE**P**GASGPMG
			218	228	238	248
			PRGPPGP**P**GK	NGDDGEAGKP	GR**P**GERGP**P**G	PQGARGL**P**GTA
RTH1	F_{11}	α_1	178	188	198	208
			GPMGPSGPRG	L**P**GP**P**GA**P**GP	QGFQGP**P**GE**P**	GE**P**GASGPMG
			218	228	238	248
			PRGPPGP**P**GK	NGDDGEAGKP	GR**P**GERGP**P**G	PQGARGL**P**GTA
	F_{21}	α_2	89	99	109	119
			GPMGLMGPRG	P**P**GASGA**P**GP	QGFQGP**P**GE**P**	GE**P**GQTGPAG
			129	139	149	159
			ARGP**P**GP**P**GK	AGEDGH**P**GKP	GR**P**GERGVVG	PQGARGF**P**GT**P**
	F_{12}	α_1	412	422	432	442
			GARGPSGPQG	PSGP**P**GPKGN	SGE**P**GA**P**GSK	GDTGAKGE**P**G
			452	462	472	482
			PTGIQGP**P**GP	AGEEGKRGAR	GE**P**GPAGL**P**G	PPGERGG**P**GSR
RTH2	F_{12}	α_1	412	422	432	442
			GARGPSGPQG	PSGP**P**GPKGN	SGE**P**GA**P**GSK	GDTGAKGE**P**G
			452	462	472	482
			PTGIQGP**P**GP	AGEEGKRGAR	GE**P**GPAGL**P**G	PPGERGG**P**GSR
	F_{22}	α_2	323	333	343	353
			GPRGI**P**GPVG	AAGATGARGL	VGE**P**GPAGS**K**	GESGNKGE**P**G
			363	373	383	393
			AVGQ**P**GP**P**GP	SGEEGKRGST	GEIGPAGP**P**G	P**P**GLRGN**P**GSR
	F_{13}	α_1	646	656	666	676
			GPAGP**P**GEAG	K**P**GEQGV**P**GD	LGA**P**GPSGAR	GERGF**P**GERG
			686	696	706	716
			VQGP**P**GPAGP	RGANGA**P**GND	GAKGDAGA**P**G	A**P**GSQGA**P**GLQ
RTH3	F_{13}	α_1	646	656	666	676
			GPAGP**P**GEAG	K**P**GEQGV**P**GD	LGA**P**GPSGAR	GERGF**P**GERG
			686	696	706	716
			VQGP**P**GPAGP	RGANGA**P**GND	GAKGDAGA**P**G	A**P**GSQGA**P**GLQ
	F_{23}	α_2	557	567	577	587
			GPAGTAGEAG	KPGERGIPGE	FGLPGPAGAR	GERGPPGESG
			597	607	617	627
			AAGPTGPIGS	RGPSGPPGPD	GNKGEPGVVG	APGTAGPSGPS
	F_{14}	α_1	880	890	900	910
			GRVG**PP**GPSG	NAGP**P**GP**P**GP	AGKEGSKGPR	GETGPAGR**P**G
			920	930	940	950
			EVGPPGP**P**GP	AGEKGA**P**GAD	GPAGA**P**GTPG	PQGIAGQRGVV

RTH4	F_{14}	α_1	880	890	900	910
			GRVG**PP**GPSG	NAGP**P**GP**P**GP	AGKEGSKGPR	GETGPAGR**P**G
			920	930	940	950
			EVGPPGP**P**GP	AGEKGA**P**GAD	GPAGA**P**GTPG	PQGIAGQRGVV
	F_{24}	α_2	791	801	811	821
			GRTGPPGPSG	ISGPPGPPGP	AGKEGLRGPR	GDQGPVGRSG
			831	841	851	861
			ETGASGPPGF	VGEKGPSGEP	GTAGPPGTPG	PQGLLGAPGFL
	F_{15}	α_1	1114	1124	1134	1144
			GLQGP**P**GP**P**G	S**P**GEQGPSGA	SGPAGPRGP**P**	GSAGSPGKDG
			1154	1165	1174	1184
			LNGL**P**GPIG**P**	**P**GPRGRTGDA	GPAG**PP**G**PP**G	**PP**GP**P**GP**P**SGG
RTH5	F_{15}	α_1	1114	1124	1134	1144
			GLQGP**P**GP**P**G	S**P**GEQGPSGA	SGPAGPRGP**P**	GSAGSPGKDG
			1154	1165	1174	1184
			LNGL**P**GPIG**P**	**P**GPRGRTGDA	GPAG**PP**G**PP**G	**PP**GP**P**GP**P**SGG
	F_{25}	α_2	1025	1035	1045	1055
			GLQGLPGLAG	HHGDQGAPGA	VGPAGPRGPA	GPSGPAGKDG
			1065	1075	1085	1095
			RIGQPGAVGP	AGIRGSQGSQ	GPAGPPGPPG	PPGPPGPSGGG

Table S3 The polypeptide fragments of F_{16}, F_{17}, F_{18} selected from α_1 chain of bovine Type I collagen (Uniport protein database, Swiss-Prot: P02453 and P02465), the polypeptide fragments of F_{26}, F_{27}, F_{28} selected from α_2 chain of bovine Type I collagen (Uniport protein database, Swiss-Prot: P02453 and P02465).

	F_{16}	α_1	850	860	870	880
			GPIGNVGA**P**G	PKGARGSAGP	**P**GATGF**P**GAA	GRVG**PP**GPSG
			890	900	910	920
			NAGP**P**GP**P**GP	AGKEGSKGPR	GETGPAGR**P**G	EVGPPGP**P**GPA
RTH6	F_{16}	α_1	850	860	870	880
			GPIGNVGA**P**G	PKGARGSAGP	**P**GATGF**P**GAA	GRVG**PP**GPSG
			890	900	910	920
			NAGP**P**GP**P**GP	AGKEGSKGPR	GETGPAGR**P**G	EVGPPGP**P**GPA
	F_{26}	α_2	761	771	781	791
			GPSGPNGPPG	PAGSRGDGGP	PGATGFPGAA	GRTGPPGPSG
			801	811	812	822
			ISGPPGPPGP	AGKEGLRGPR	GDQGPVGRSG	ETGASGPPGFV
	F_{17}	α_1	616	626	636	646
			GAQGP**P**GPAG	PAGERGEQGP	AGS**P**GFQGL**P**	GPAG**P**PGEAG
			656	666	676	686
			K**P**GEQGV**P**GD	LGA**P**GPSGAR	GERGF**P**GERG	VQGP**P**GPAGPR
	F_{17}	α_1	616	626	636	646
RTH7			GAQGP**P**GPAG	PAGERGEQGP	AGS**P**GFQGL**P**	GPAG**P**PGEAG
			656	666	676	686
			K**P**GEQGV**P**GD	LGA**P**GPSGAR	GERGF**P**GERG	VQGP**P**GPAGPR
	F_{27}	α_2	527	537	547	557
			GAQGPPGLQG	VQGGKGEQGP	AGPPGFQGLP	GPAGTAGEAG
			567	577	587	597
			KPGERGIPGE	FGLPGPAGAR	GERGPPGESG	AAGPTGPIGSR
	F_{18}	α_1	382	392	402	412
			GPAGN**P**GADG	Q**P**GAKGANGA	**P**GIAGA**P**GF**P**	GARGPSGPQG
			422	432	442	452
			PSGP**P**GP**K**GN	SGE**P**GA**P**GSK	GDTGAKGE**P**G	PTGIQGP**P**GPA
	F_{18}	α_1	382	392	402	412
RTH8			GPAGN**P**GADG	Q**P**GAKGANGA	**P**GIAGA**P**GF**P**	GARGPSGPQG
			422	432	442	452

		PSGP**P**GP**K**GN	SGE**P**GA**P**GSK	GDTGAKGE**P**G	PTGIQGP**P**GPA
F_{28}	α_2	293	303	313	323
		GP**P**GNPGANG	L**P**GAKGAAGL	**P**GVAGA**P**GL**P**	GPRGI**P**GPVG
		333	343	353	363
		AAGATGARGL	VGE**P**GPAGS**K**	GESGNKGE**P**G	AVGQ**P**GP**P**GPS

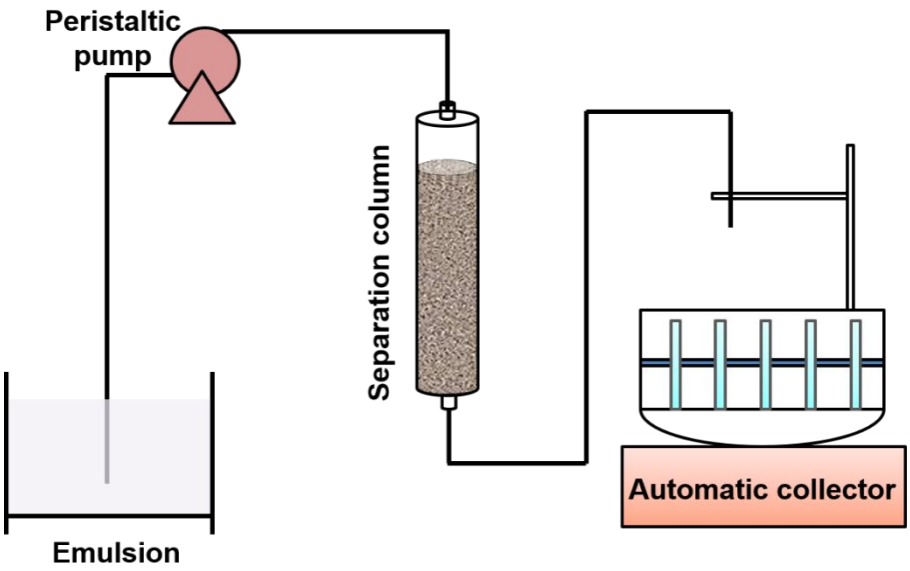

Schematic illustration S1 The emulsion separation system. Emulsions were pumped into the column packed with collagen fibers through the plastic tubes by the peristaltic pump, and the filtrates were collected by the automatic collector after the separation by collagen fibers.

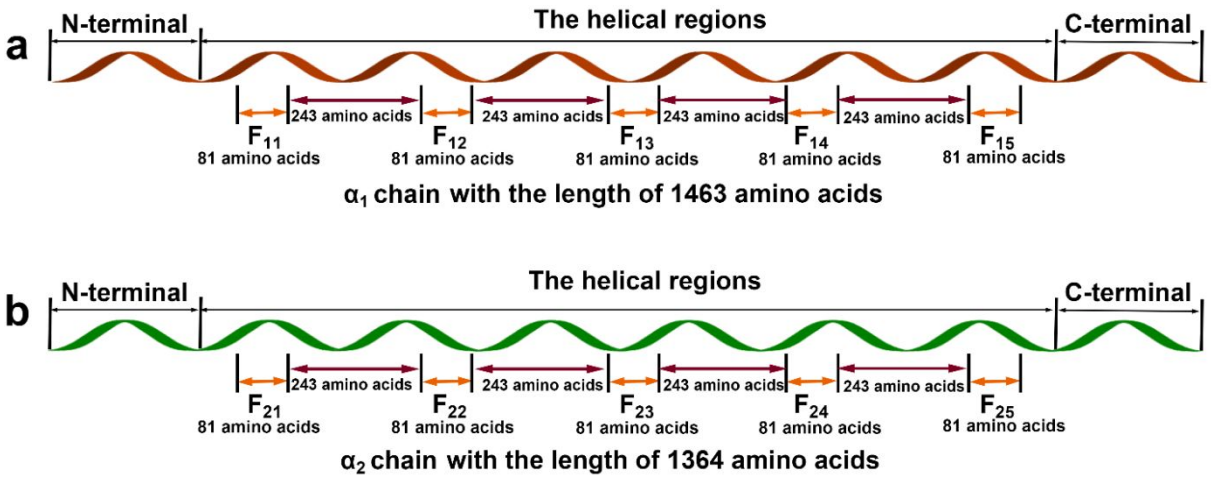

Schematic illustration S2 Illustration shows the selection of polypeptide fragments from α_1 and α_2 chains for constructing collagen fiber model. Five polypeptide fragments of F_{11}, F_{12}, F_{13}, F_{14}, F_{15} selected from α_1 chain of bovine Type I collagen molecule (a) and five polypeptide fragments of F_{21}, F_{22}, F_{23}, F_{24}, F_{25} selected from α_2 chain of bovine Type I collagen molecule (b). Each of the selected polypeptide fragments had the length of 81 amino acids, with an interval of the length of 243 amino acids between two adjacent fragments.

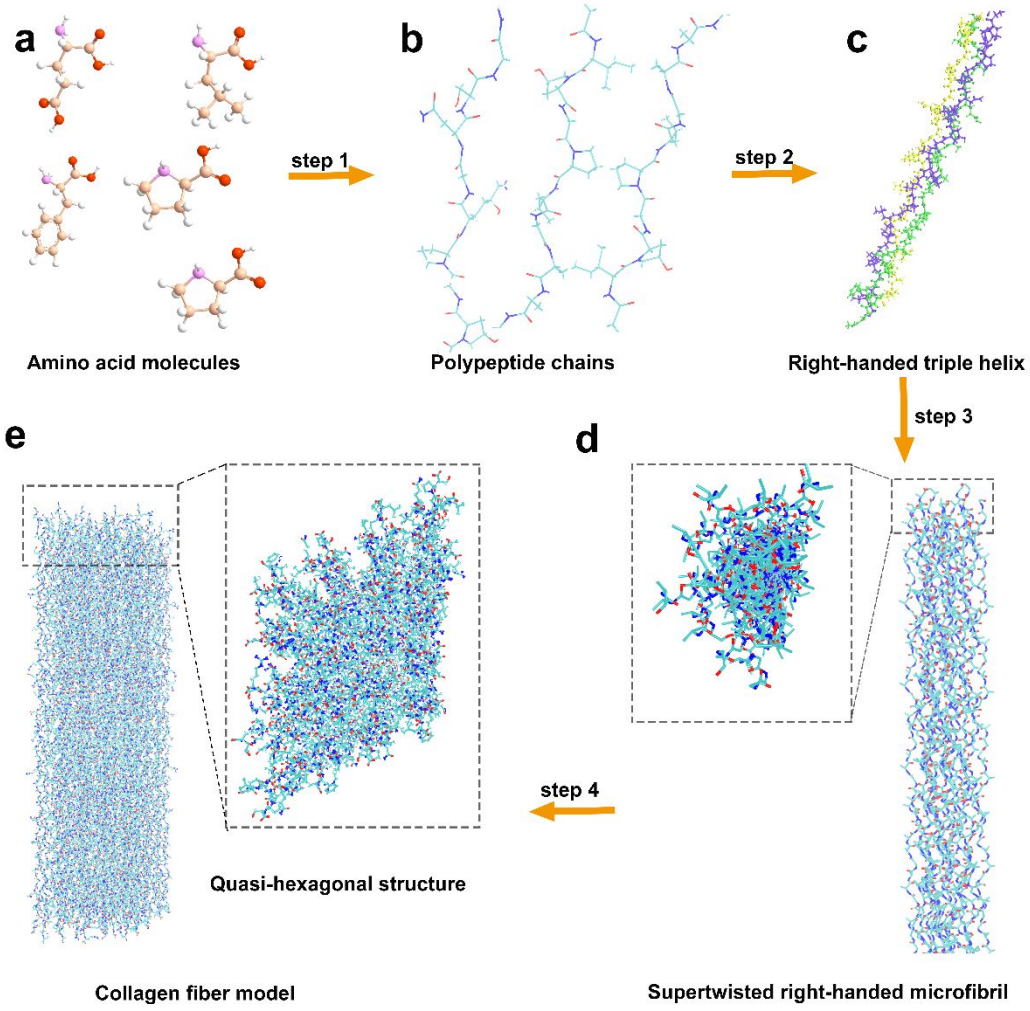

Schematic illustration S3 Illustration shows the process to construct the collagen fiber model. Step 1: the polypeptide chains (b) were constructed using the amino acid sequences of selected polypeptide fragments of α_1 and α_2 chains of bovine Type I collagen molecule (a), step 2: three polypeptide chains were twisted together into a right-handed triple helix (c), step 3: five right-handed triple helices were packed to from a supertwisted right-handed microfibril (d), step 4: four identical supertwisted right-handed microfibrils were bundled to form the collagen fiber model, with a quasi-hexagonal arrangement of all the comprised of triple helixes (e).

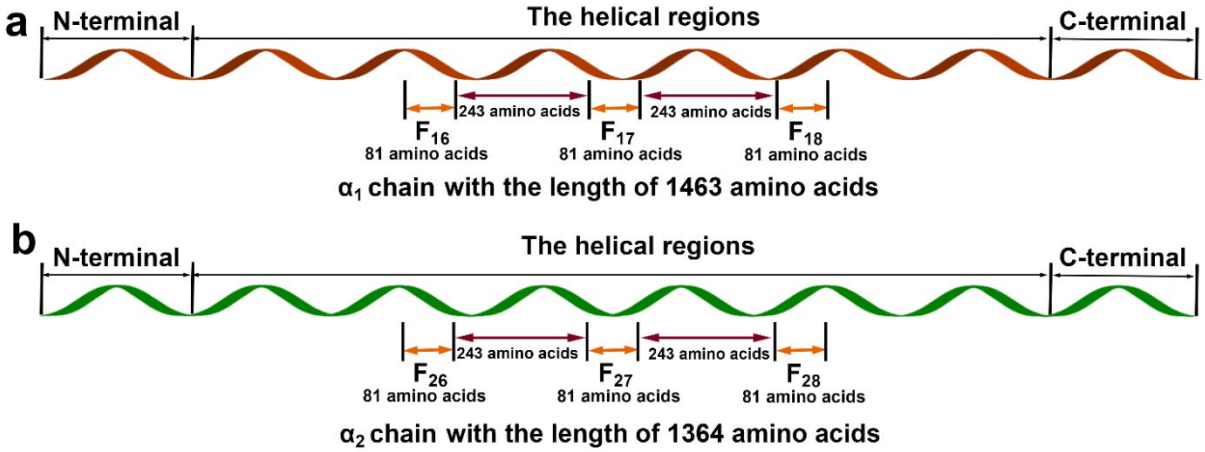

Schematic illustration S4 Illustration shows the selection of polypeptide fragments from α1 and α2 chains for constructing the simplified collagen fiber model. Three polypeptide fragments of F_{16}, F_{17}, F_{18} selected from α_1 chain of bovine Type I collagen molecule (a) and three polypeptide fragments of F_{26}, F_{27}, F_{28} selected from α_2 chain of bovine Type I collagen molecule (b). Each of the selected polypeptide fragments had the length of 81 amino acids, with an interval of the length of 243 amino acids between two adjacent fragments.

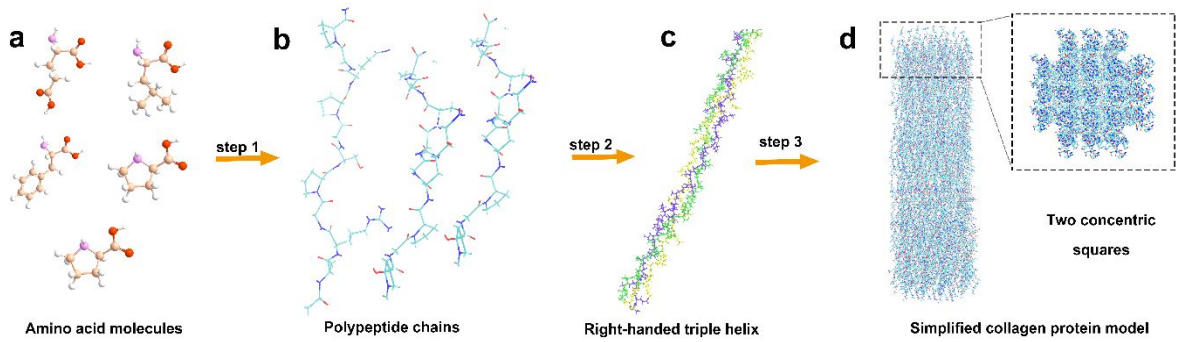

Schematic illustration S5 Illustration shows the process to construct the simplified collagen fiber model. Step 1: the polypeptide chains (b) were constructed using amino acid sequences of selected fragments of α_1 and α_2 chains of bovine Type I collagen molecule (a), step 2: three polypeptide chains were twisted together into a right-handed triple helix (c), step 3: twenty one right-handed triple helixes were parallelly arranged in the two concentric squares to form the simplified collagen fiber model, in which one RTH6 was located in the center of square, eight identical RTH7 were located around four sides of the inner square, and twelve identical RTH8 were arranged around four sides of the external square, respectively (d).

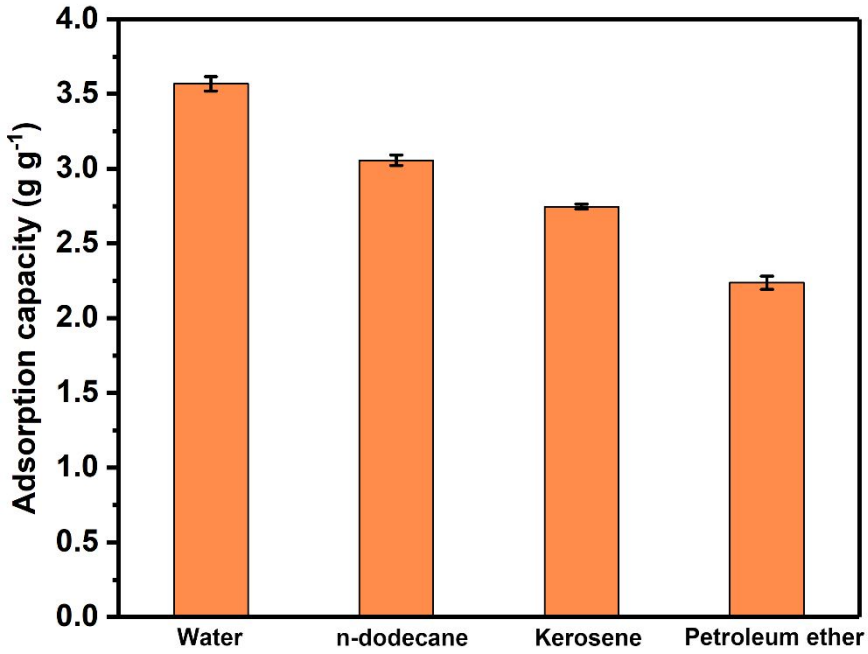

Figure S1 Adsorption capacity of collagen fibers with respect to water, n-dodecane, kerosene and petroleum ether, respectively.

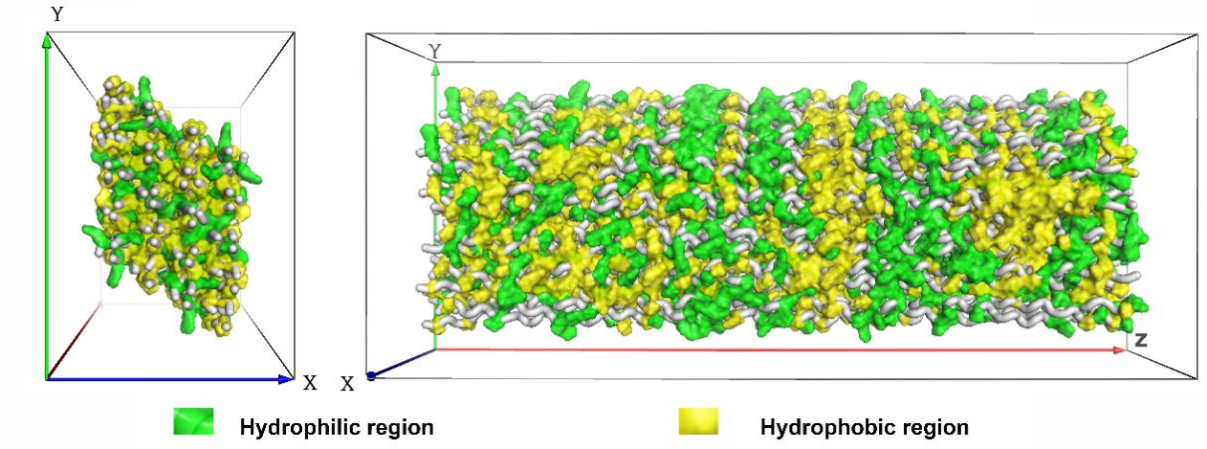

Figure S2 Images showing the collagen fiber model.

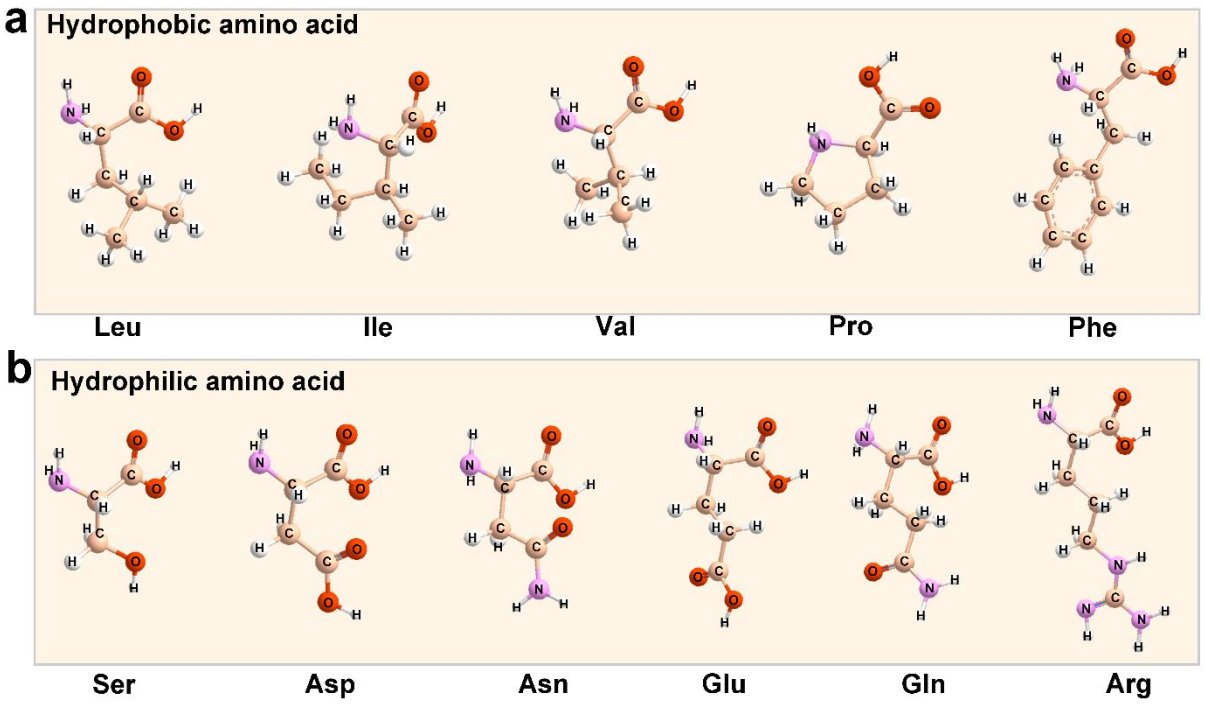

Figure S3 The hydrophobic (a) and hydrophilic (b) amino acids that comprise the collagen fiber model.

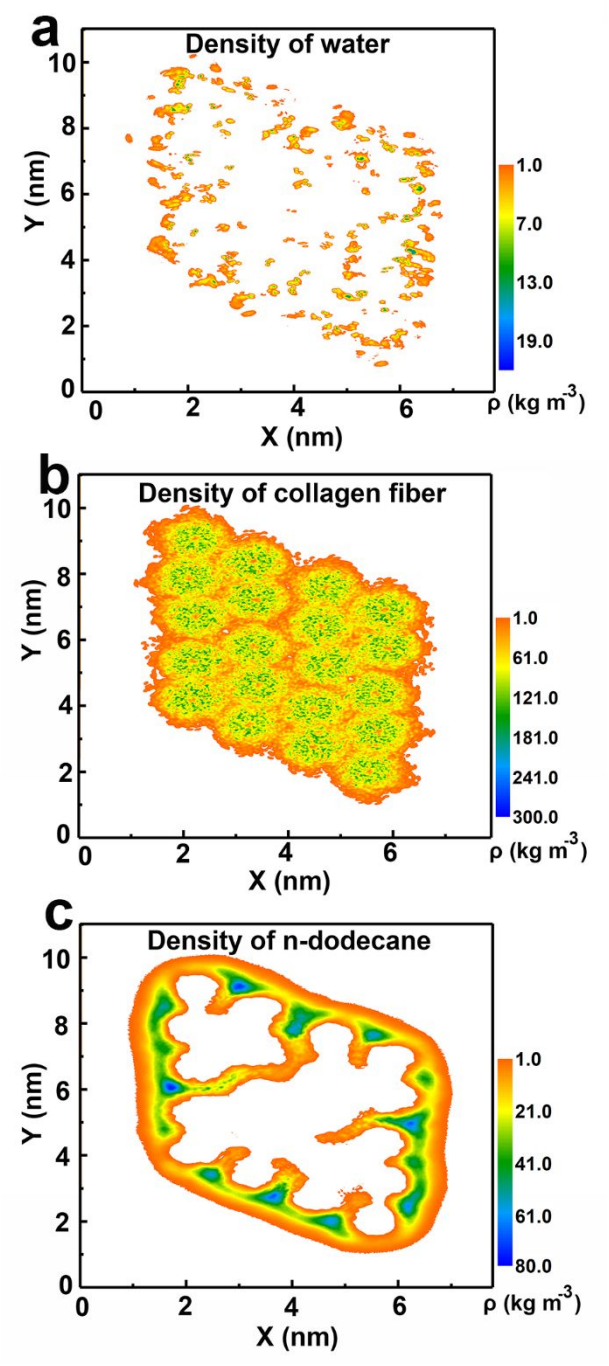

Figure S4 The cross-section density distribution of water molecules (a), collagen fiber (b) and n-dodecane molecules (c) at 20 ns in simulation 1.

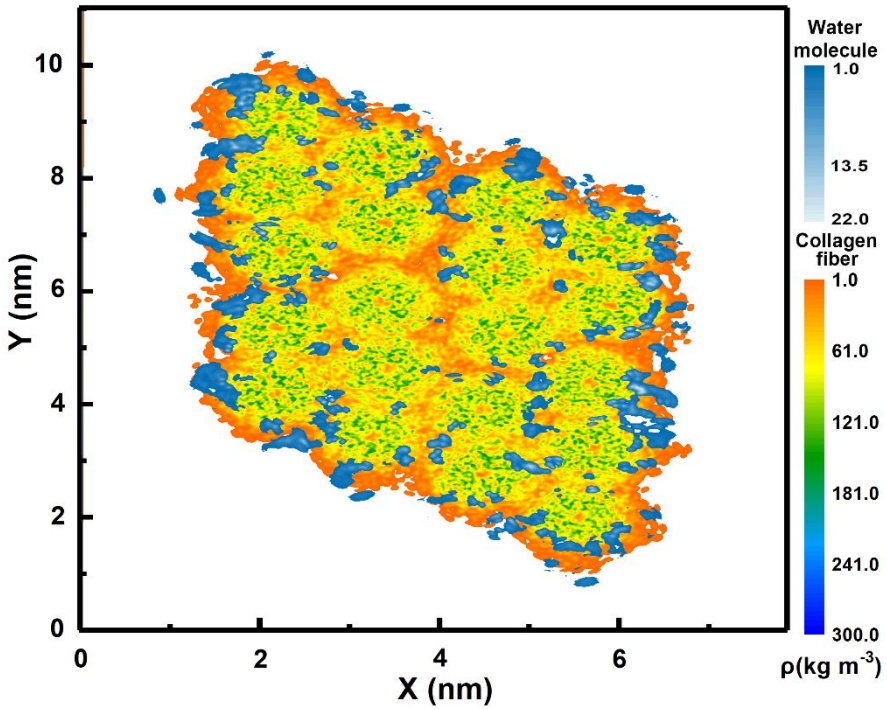

Figure S5 Cross-section density distributions of water molecules and collagen fiber at 20 ns in the simulation 1.

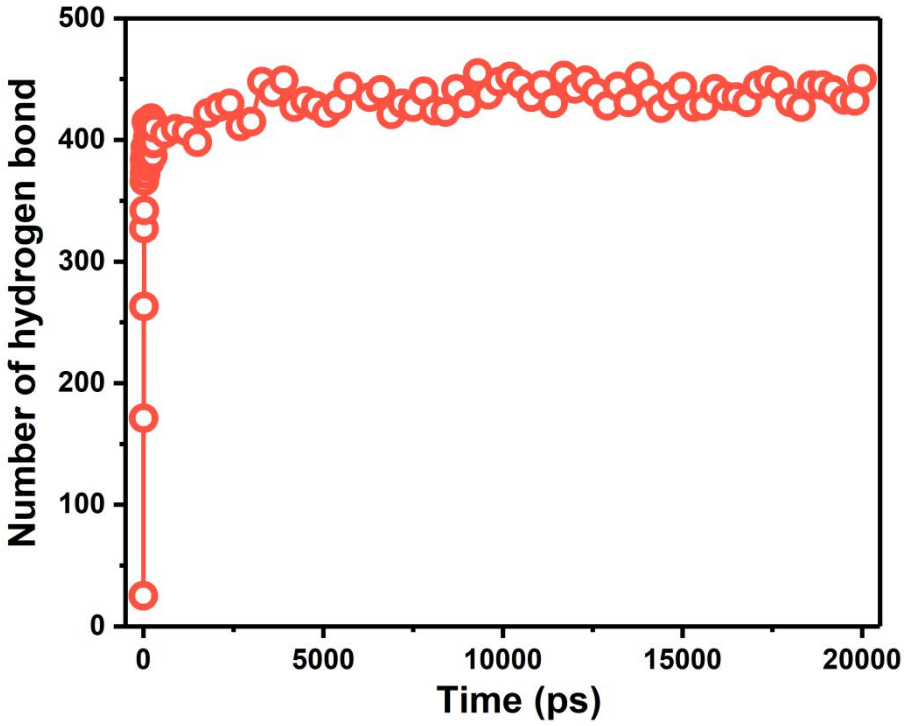

Figure S6 Number of hydrogen bond formed during the simulation 1.

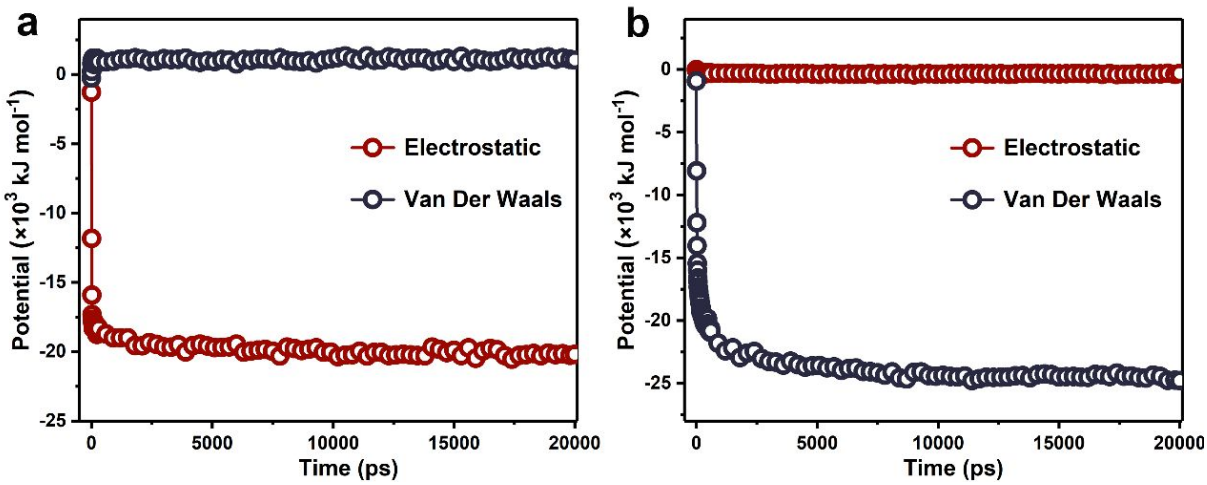

Figure S7 Calculated electrostatic and Van Der Waals potentials between water molecules and collagen fiber model during the simulation 1 (a), calculated electrostatic and Van Der Waals potentials between n-dodecane molecules and collagen fiber model during the simulation 1 (b).

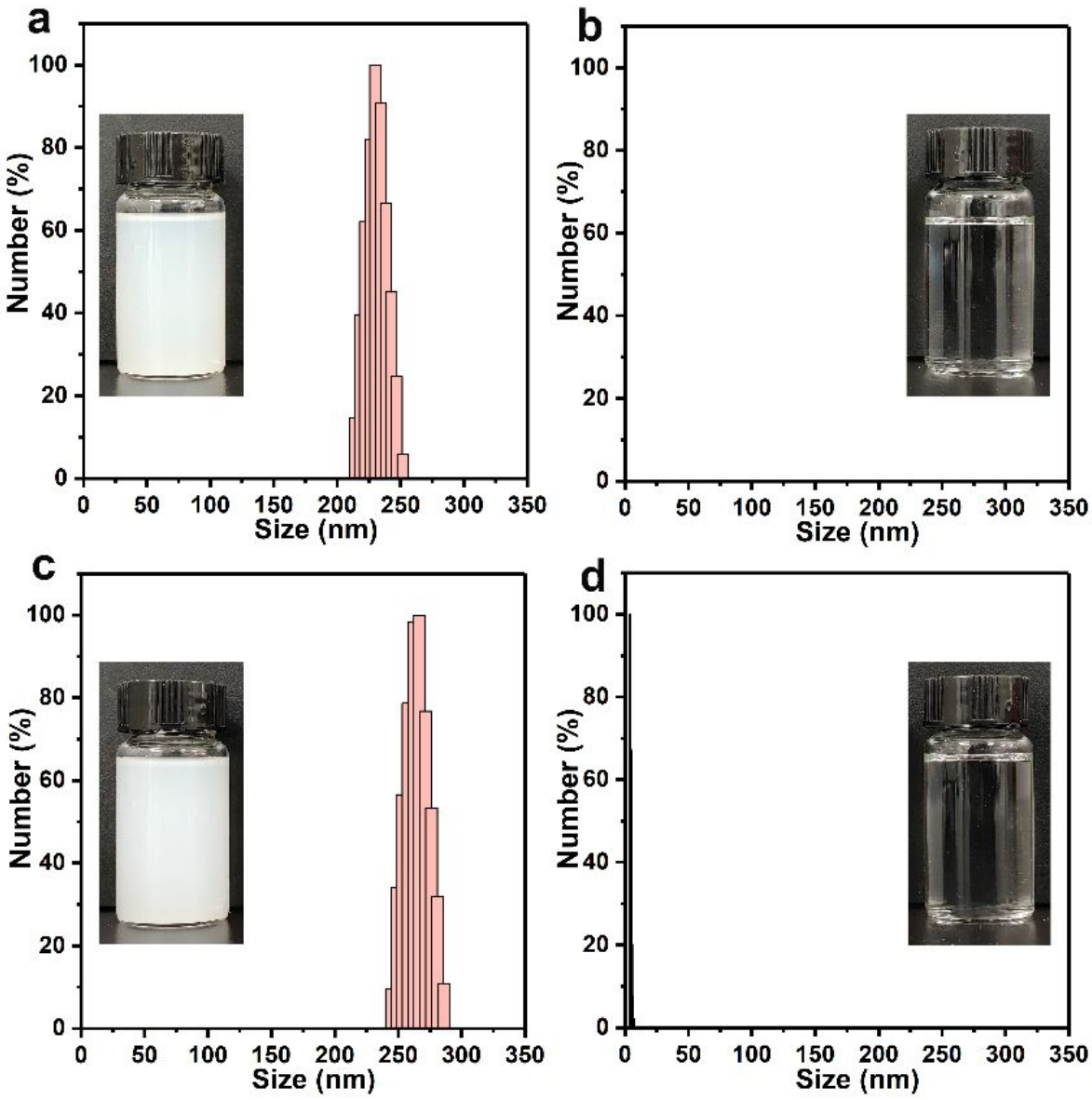

Figure S8 DLS curves of E2 before (a) and after (b) the separation by collagen fibers (the insets in a and b are the corresponding digital photos, respectively), DLS curves of E3 before (c) and after (d) the separation by collagen fibers (the insets in c and d are the corresponding digital photos, respectively).

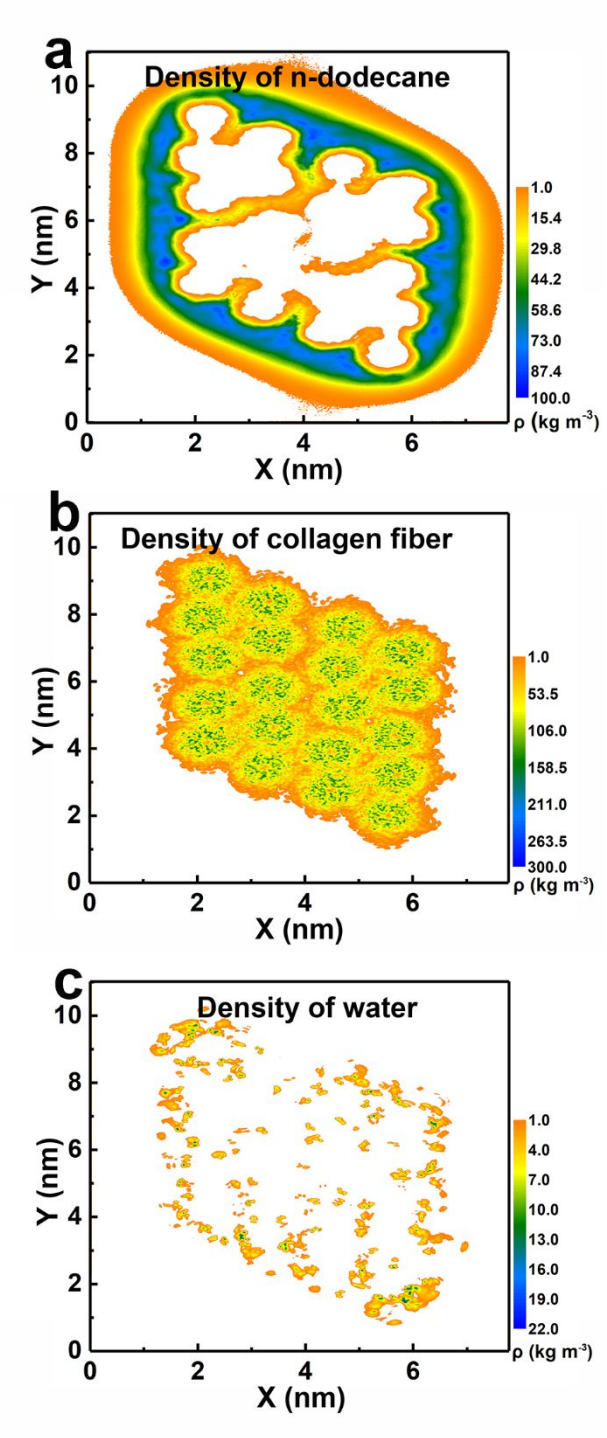

Figure S9 The cross-section density distribution of n-dodecane molecules (a), collagen fiber (b) and water molecules (c) at 20 ns in simulation 2.

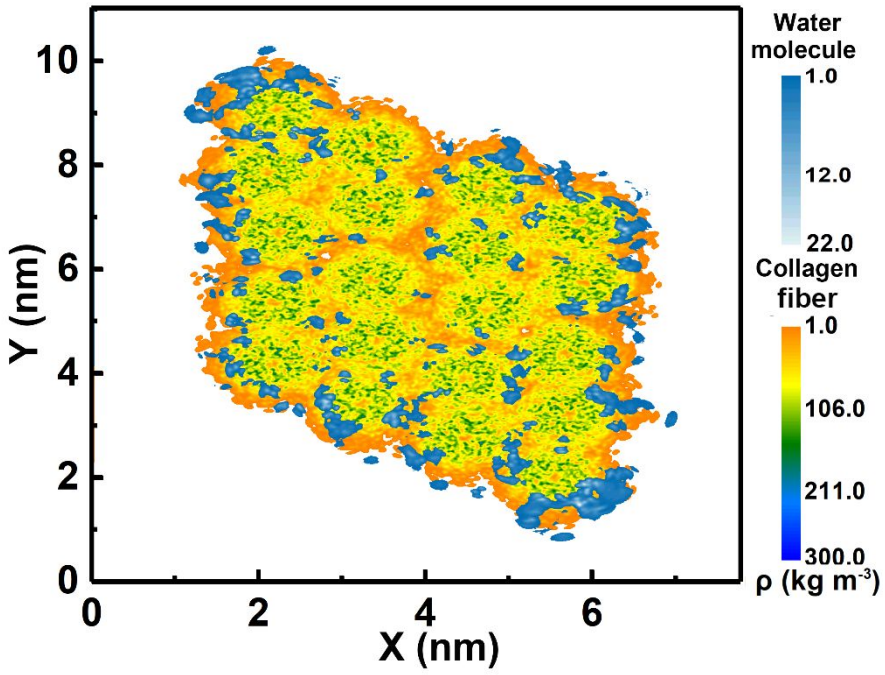

Figure S10 Cross-section density distributions of water molecules and collagen fiber at 20 ns in the simulation 2.

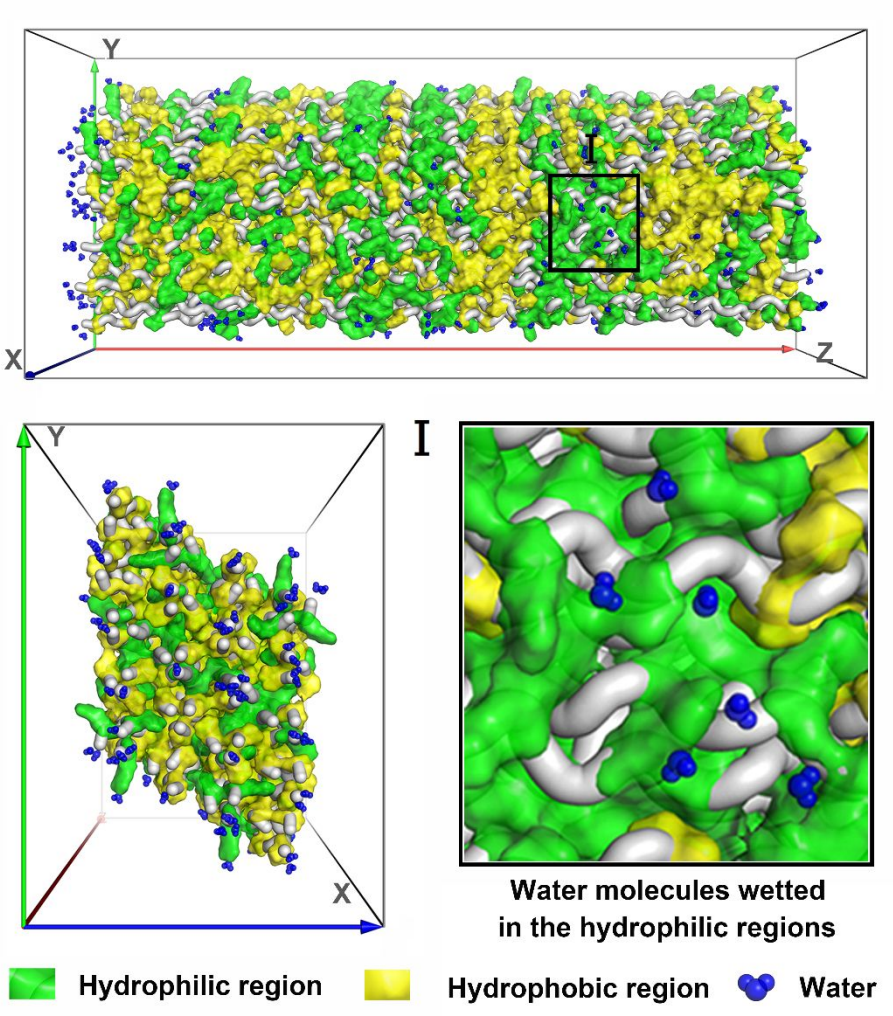

Figure S11 Images showing the regional wetting of 300 water molecules in the hydrophilic regions of collagen fiber model at 20 ns in simulation 2, and the magnified area I.

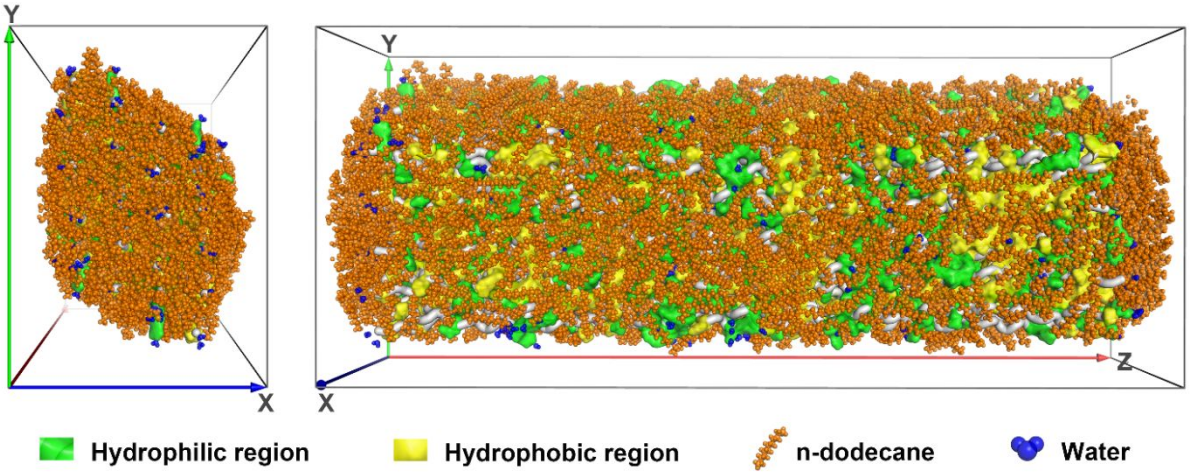

Figure S12 Images of the collagen fiber model wetted by 300 water and 1162 d-dodecane molecules at 20 ns in simulation 2.

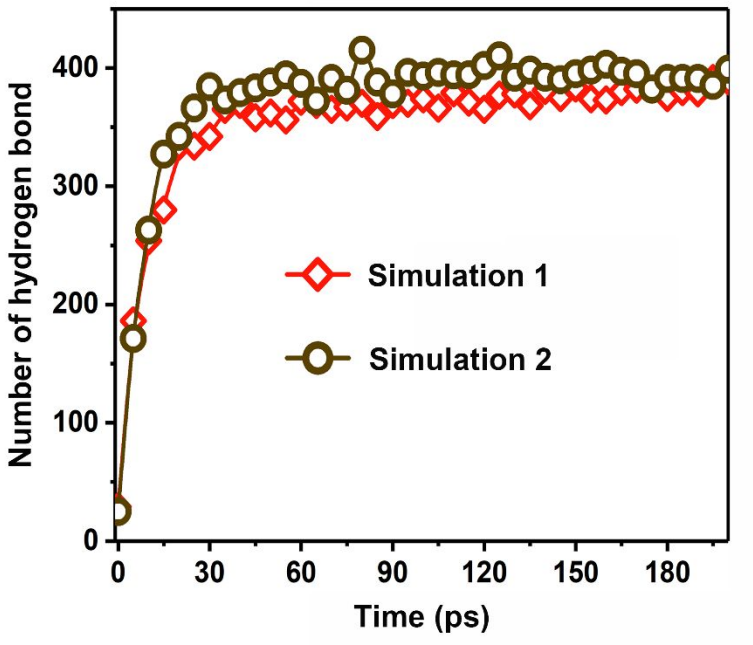

Figure S13 Number of hydrogen bond formed during the simulation 1 and simulation 2, respectively.

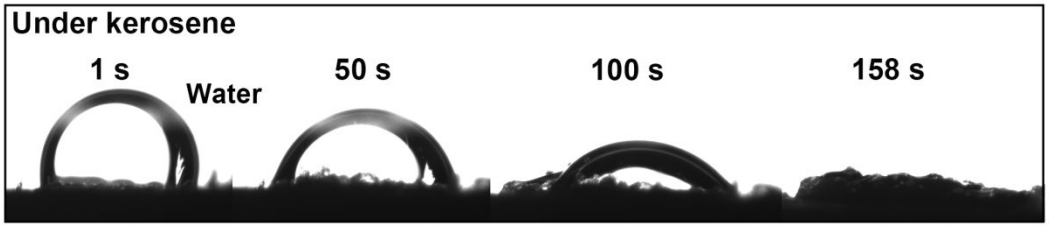

Figure S14 Images of water contact angle showing the permeation of water droplet into collagen fibers under kerosene.

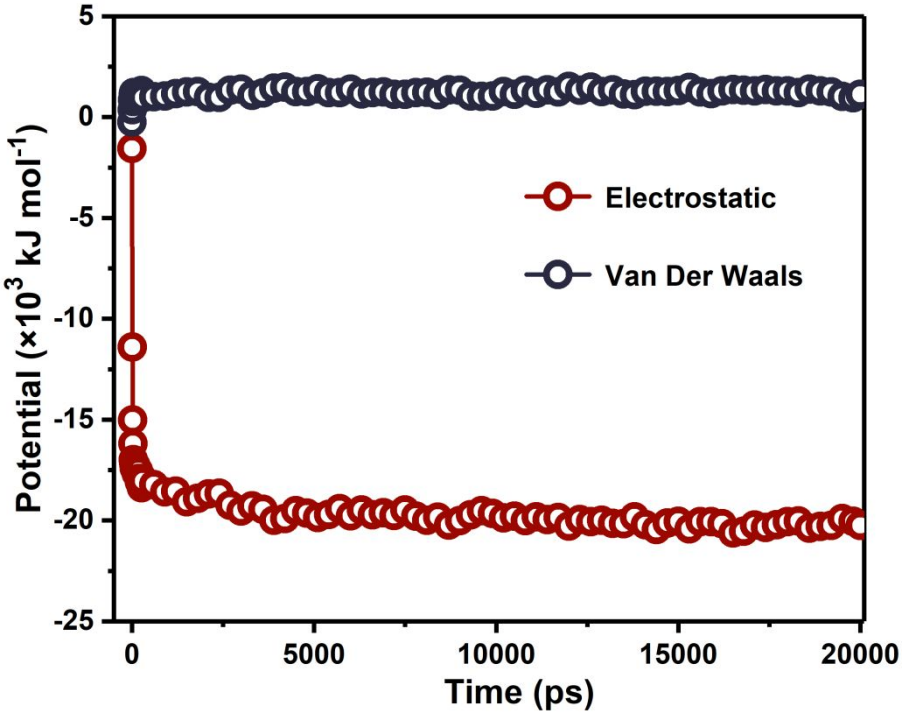

Figure S15 Calculated electrostatic potential and Van Der Waals potentials between water molecules and collagen fiber model during the simulation 2.

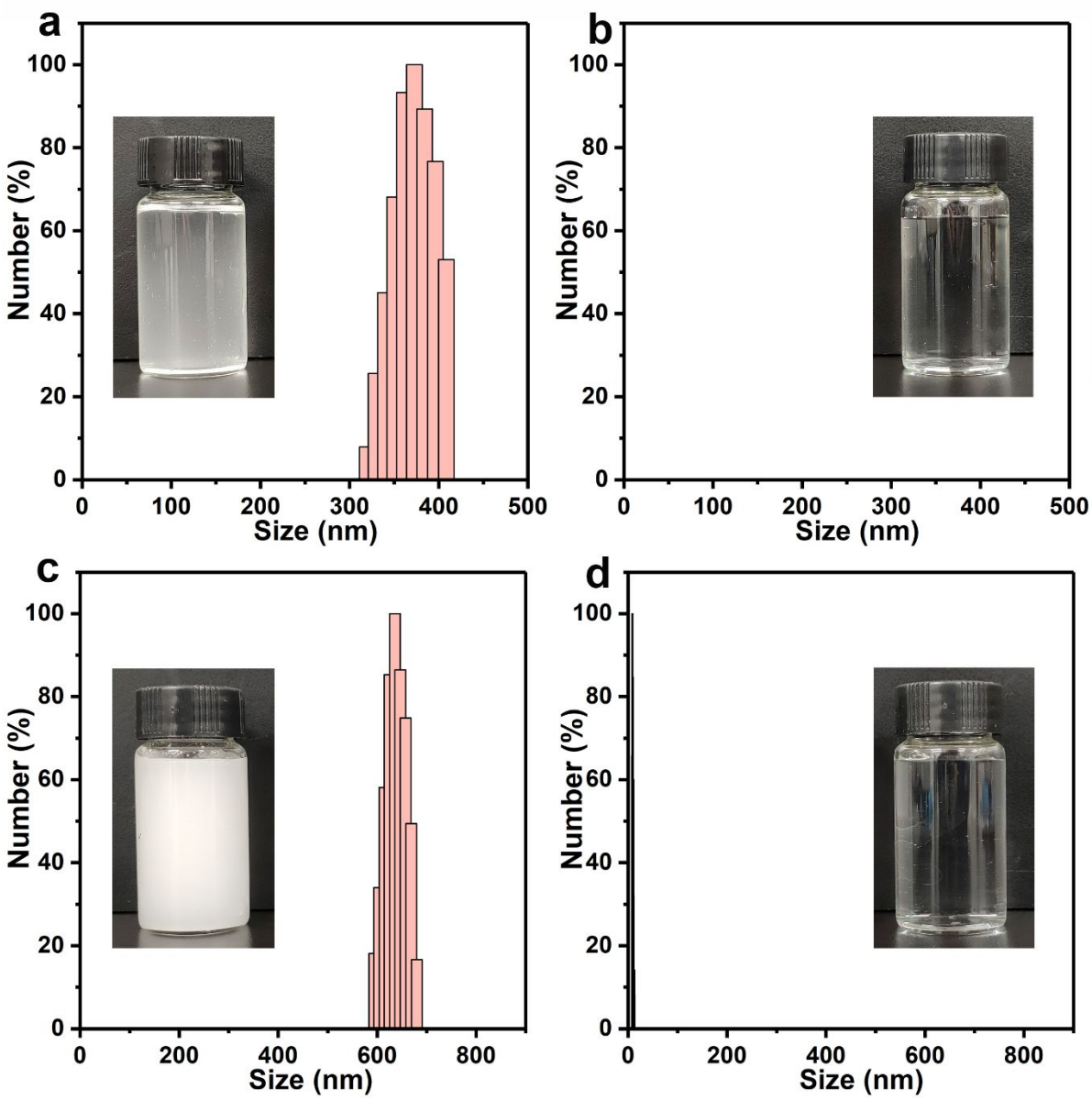

Figure S16 DLS curves of E6 before (a) and after (b) the separation by collagen fibers (the insets in a and b are the corresponding digital photos, respectively), DLS curves of E7 before (c) and after (d) the separation by collagen fibers (the insets in c and d are the corresponding digital photos, respecively).

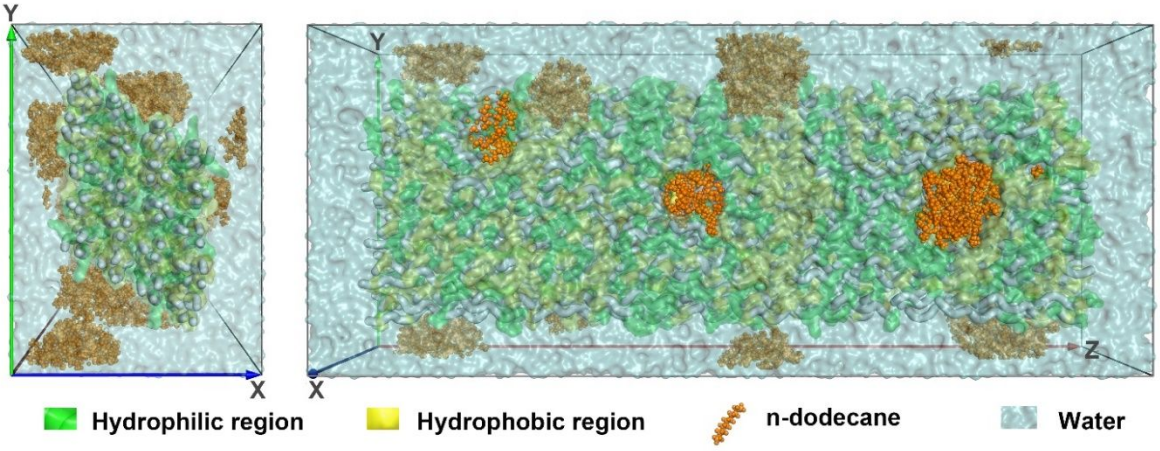

Figure S17 Images of the collagen fiber model wetted by 300 n-dodecane and 52926 water molecules at 20 ns in simulation 3.

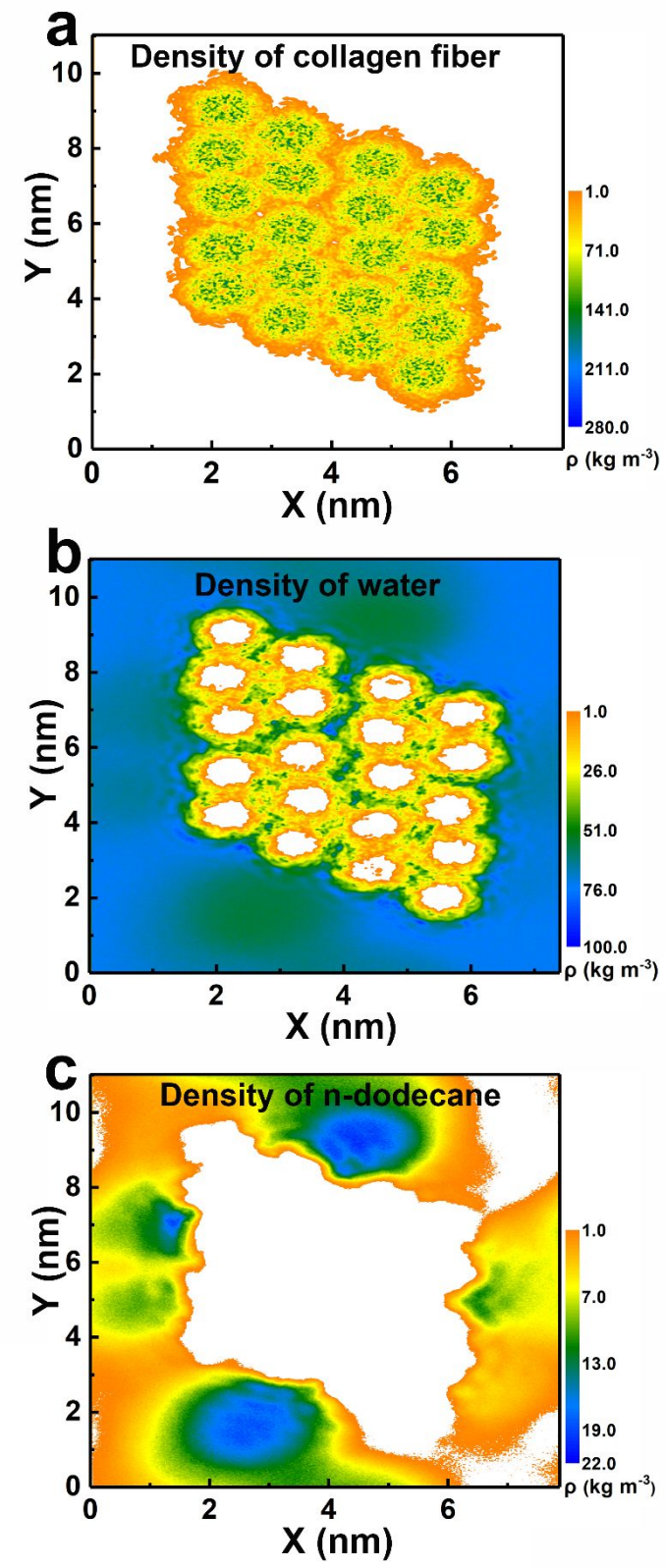

Figure S18 The cross-section density distribution of collagen fiber (a), water molecules (b) and n-dodecane molecules (c) at 20 ns in simulation 3.

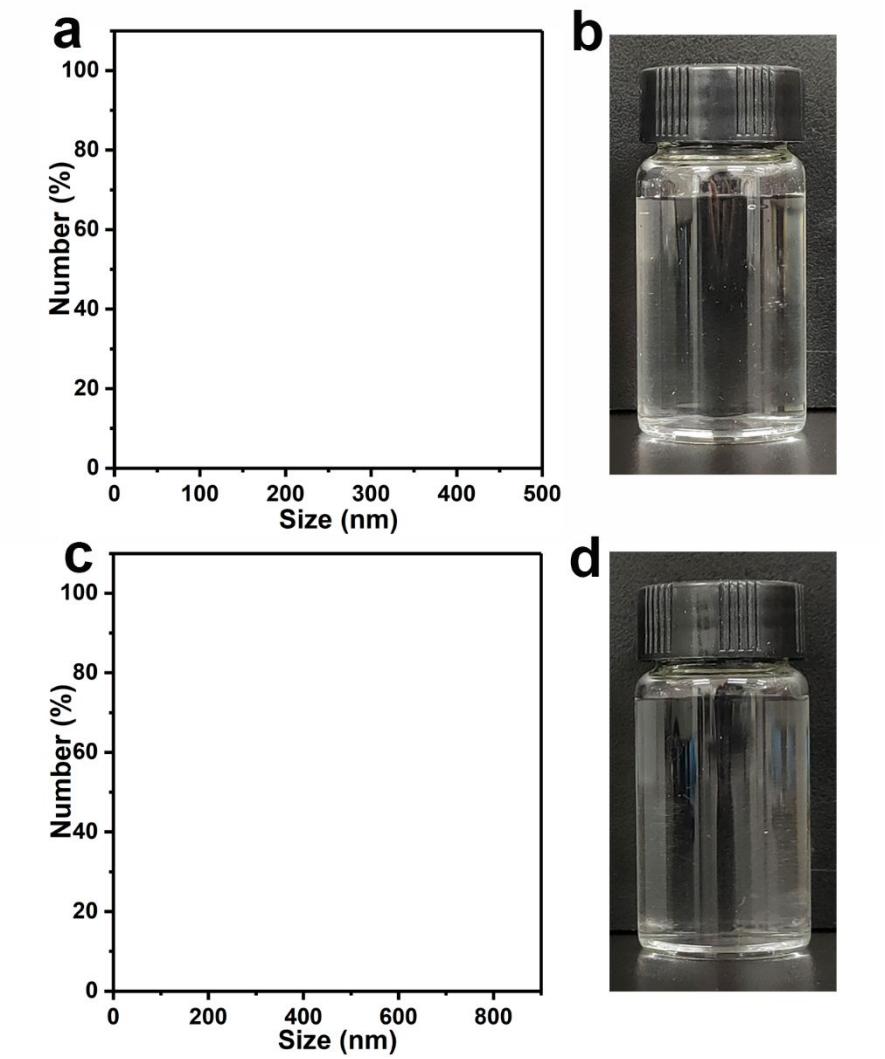

Figure S19 DLS curves of E6 (a) and E7 (c) after the separation by collagen fibers with the pre-wetting of water, digital photos of E6 (b) and E7 (d) after the separation by collagen fibers with the pre-wetting of water.

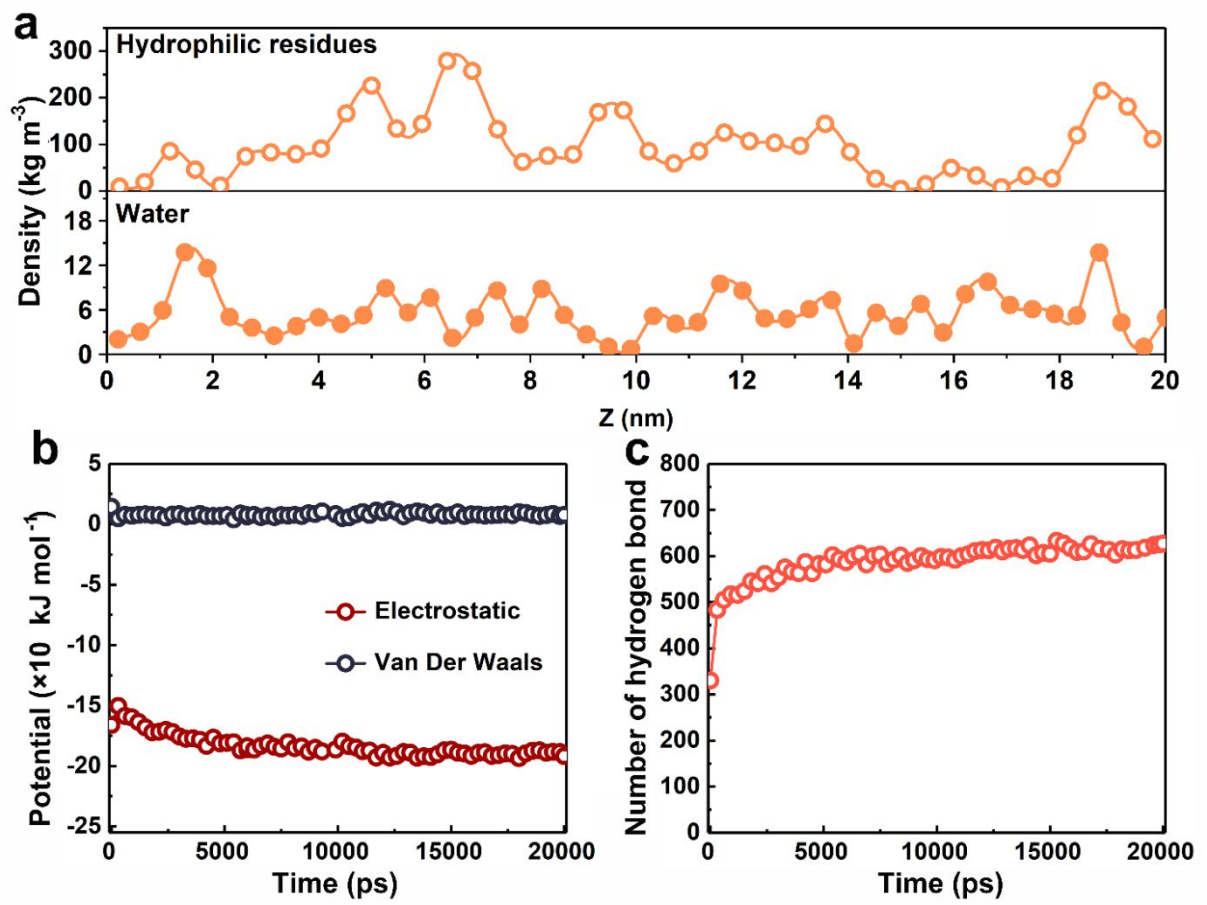

Figure S20 Longitudinal density distribution of water molecules and hydrophilic residuals of simplified collagen fiber model at 20 ns in simulation 5 (a), calculated electrostatic and Van Der Waals potentials between water molecules and the simplified collagen fiber model during the simulation 5 (b), number of hydrogen bond formed between the simplified collagen fiber model and water molecules during the simulation 5 (c).

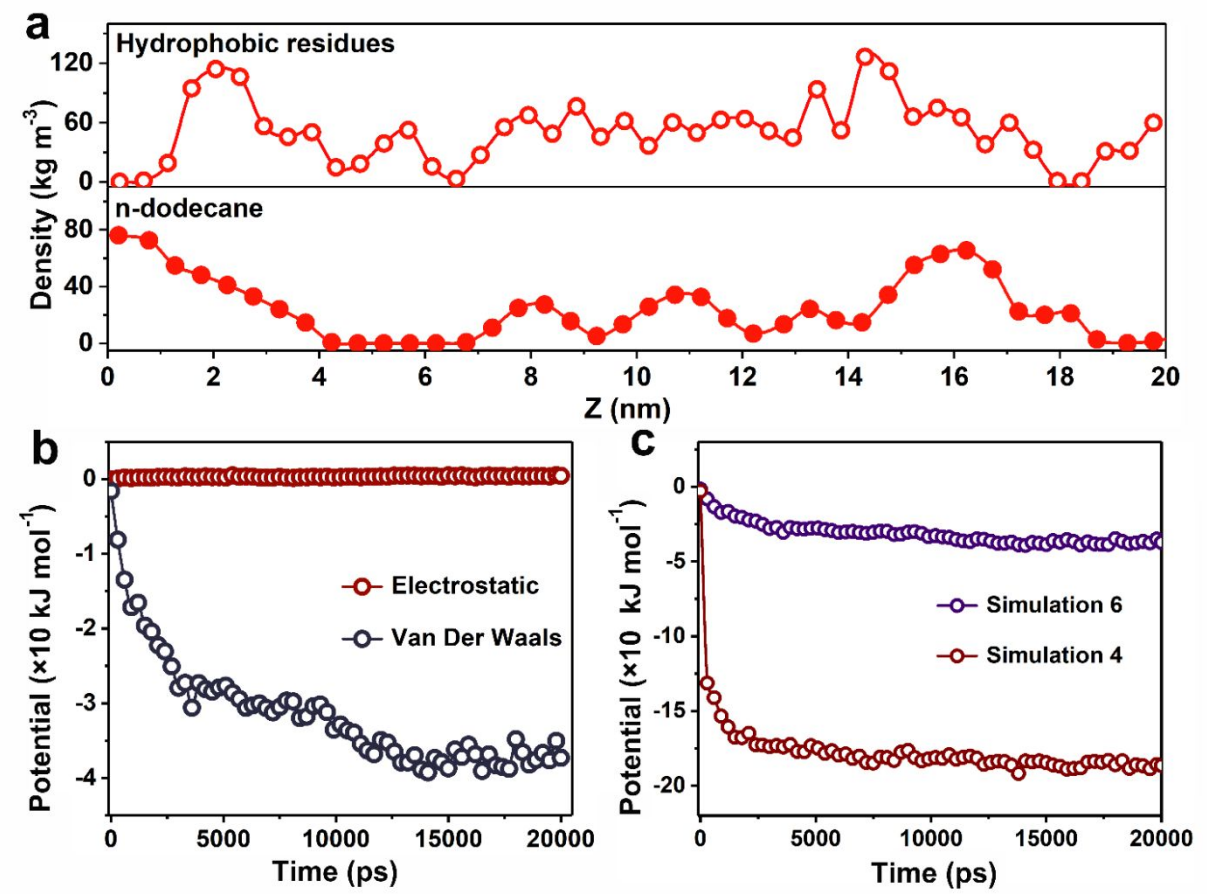

Figure S21 Longitudinal density distribution of n-dodecane molecules and hydrophobic residuals of simplified collagen fiber model at 20 ns in simulation 6 (a), calculated electrostatic and Van Der Waals potential between n-dodecane molecules and the simplified collagen fiber model during the simulation 6 (b), calculated Van Der Waals potential between n-dodecane molecules and the simplified collagen fiber model during the simulation 4 and simulation 6 (c).